International Journal on Advanced Science Engineering Information Technology

Vol.14 (2024) No. 4
ISSN: 2088-5334

Enhanced Non-Orthogonal Multiple Access Performance Using Channel Coding for High-Altitude Platform System (HAPS)

Veronica Windha Mahyastuty [a,*], Theresia Ghozali [a], Sandra Octaviani [a], Brian Pamukti [b]

[a] *Electrical Engineering Department, Atma Jaya Catholic University of Indonesia, Jend. Sudirman Street No. 51, Jakarta, Indonesia*
[b] *School of Electrical Engineering, Telkom University, Telekomunikasi Street No.1, Bandung, Indonesia*

*Corresponding author: *veronica.may@atmajaya.ac.id*

***Abstract*—The high-altitude platform system (HAPS) is a promising technology for providing high-speed data transmission and coverage for remote areas. Still, it suffers from unpredictable channel transmission, especially in the Rician channel. To overcome the issue in transmission, we used one channel coding strategy, namely the quasi-cyclic low-density parity-check (QC-LDPC). This study aims to evaluate the performance of power domain non-orthogonal multiple access (PD-NOMA), which allows multiple users to share the same spectrum in a downlink communication system from HAPS to three ground stations. We simulated the system using MATLAB simulation with different power allocation coefficients for every ground station. The simulation results showed that QC-LDPC codes can significantly lower the signal-to-noise ratio (SNR) required to achieve the same bit error rate (BER) as uncoded NOMA, especially in scenarios with uneven power allocation. The average improvement of QC-LDPC over uncoded NOMA was 8.4% in SNR. However, we also observed that NOMA is prone to domino errors, where decoding errors in one ground station can propagate and degrade the performance of the subsequent ground station. Furthermore, we found that power allocation significantly impacts the system performance, while the location and power allocation of the second ground station have a minor effect. Based on these findings, we conclude that QC-LDPC can enhance system performance in scenarios with low received power and that power allocation is a crucial factor for NOMA systems with multiple ground stations.**

***Keywords*—Channel coding; communication; high altitude platform system; low-density parity-check; non-orthogonal multiple access.**

Manuscript received 15 Oct. 2020; revised 29 Jan. 2021; accepted 2 Feb. 2021. Date of publication 31 Aug. 2024.

I. INTRODUCTION

A high-altitude platform system (HAPS) comprises various aircraft operating within the stratosphere, such as planes, balloons, and airships, located approximately 12 to 50 kilometers above the earth's surface. These vehicles have communication and surveillance devices and possess extended-duration power sources to sustain prolonged flight at high altitudes [1], [2], [3], [4]. HAPS technology finds diverse applications, spanning communications, surveillance, environmental monitoring, and disaster response. In the realm of communications, it facilitates wireless broadband access in remote regions and extends cellular network reach. In surveillance, HAPS serves border control, maritime surveillance, and disaster tracking. For environmental monitoring, it gathers vital data on weather, air quality, and climate shifts [5], [6], [7], [8].

HAPS offers numerous advantages over conventional satellite systems. They enable rapid deployment, easy relocation, extensive coverage, and enhanced data capacity compared to ground-based systems. Furthermore, HAPS exhibit greater resilience to adverse weather conditions and can access remote and challenging-to-reach locations [9], [10], [11].

However, HAPS technology also encounters challenges such as obtaining regulatory approval, resolving technical issues related to operating at high altitudes, and avoiding interference with planes and other wireless systems. Despite these challenges, HAPS technology is anticipated to be vital in delivering essential communication 6G and surveillance services in the future [12], [13], [14], [15].

In recent years, unmanned aerial vehicles (UAVs) have emerged as a potent data collection and communication tool. Researchers [16], [17], [18], [19] conducted a study to investigate the role of UAVs in data capture and transmission. The UAVs flew above the earth, collecting and inputting data into a database focusing on optimizing accuracy through machine learning. However, a crucial aspect left unexplored in this study pertained to the communication process necessary for transmitting collected data or results to other UAVs or ground stations.

In their study [20], [21], [22], researchers analyzed the challenges and solutions associated with 5G channel coding schemes. They offer a comprehensive overview of 5G technology's latest advancements and their implications for channel coding. The study delves into the complex coding challenges of 5G, scrutinizes key channel code options, and explores their adaptations for 5G use. The researchers also pinpointed research gaps and proposed future 5G channel coding directions [23].

The paper by [24] examined the impact of transmit antenna selection (TAS) on a non-orthogonal multiple access (NOMA-based) integrated satellite-HAP-terrestrial network with imperfect channel state information (CSI) and successive interference cancellation (SIC). The authors devise a TAS algorithm that balances the signal-to-interference-plus-noise ratio (SINR) and the rate of user demands. Simulations show that TAS can boost the system's capacity and the user's achievable rates. Moreover, the simulations demonstrate that the proposed algorithm surpasses the conventional TAS algorithms, especially with imperfect CSI and SIC. The paper emphasizes the role of TAS in improving the performance of NOMA-based networks and offers valuable insights into the design and optimization of future communication systems [25].

Researchers [26] proposed a broadband communication system for high-speed flying devices that use soft 4-quadrature amplitude modulation (QAM) modulation, orthogonal frequency division multiplexing (OFDM) with second-generation digital terrestrial television broadcasting system (DVB-T2) LDPC codes, and minimum mean squared error (MMSE) equalization. The system achieved better bit error rate (BER) performance, lower error floor, and higher maximum speed than uncoded and hard-decision systems under additive white Gaussian noise (AWGN) and multipath Rayleigh fading channels. The system also faces challenges such as complexity, phase noise, timing offset, adaptive modulation and coding, and compatibility with existing standards.

In a recent study by [27] explored the effectiveness of employing the Golay code in HAPS communication, comparing it with uncoded information. The study presents compelling evidence that the proposed link budget and channel model effectively address critical challenges in HAPS communication, including high BER, low time delay, and inefficient channel transmission. Simulation results underscore that increasing the signal-to-noise ratio yields substantial gains and enhanced HAPS link transmission power. Moreover, the study emphasizes the benefits of channel coding, with the Golay code outperforming the uncoded version in terms of BER. In addition, the Rician channel and the coding strategy were analyzed, but no multiple access technique was used in HAPS.

In this paper, we investigate a method for enhancing the performance of a NOMA system with quasi-cyclic low-density parity-check (QC-LDPC) codes in a downlink communication system with a HAPS and three gateways. NOMA is a technique that allows multiple users to share the same spectrum by using different power levels, while QC-LDPC codes are error-correcting codes that can improve the reliability of the transmission. HAPS is a promising technology for sending data but suffers from unpredictable channel transmission, especially on the Rician channel. Our main contributions are summarized as follows:

- To the best of our knowledge, we are the first to investigate the combination of Rician channel, QC-LDPC codes, and power domain NOMA for HAPS communication, as previous studies only considered one or two of these aspects.
- We demonstrate that QC-LDPC codes can significantly lower the signal-to-noise ratio (SNR) required to achieve the same BER as uncoded NOMA, especially in scenarios with uneven power allocation or diverse channel gains.
- We provide valuable insights into the role of coding schemes and power allocation in NOMA systems and suggest potential future research and improvement areas.

This paper comprises four main sections. In the second section, we offer an insight into the block diagram of our proposed communication system, encompassing key components like encoder LDPC, superposition coding (SPC), Rician channel, SIC, and decoder. We also provide a comprehensive breakdown of the variables and scenarios central to our study. Moving on to the third section, we present the outcomes of our extensive simulations and elucidate the figures that depict our system's performance. Lastly, the concluding section of this paper encapsulates the research's key findings and conclusions.

II. Materials and Method

This section presents the block diagram and graphical representation of our HAPS-NOMA study using QC-LDPC codes. We describe each communication system component, from the transmitter to the receiver. We explain the encoding and decoding processes with QC-LDPC codes. We also discuss superposition coding, which allows multiple users to share the same time-frequency resources in NOMA. Moreover, we show the communication system and the simulation methodology in a visual form.

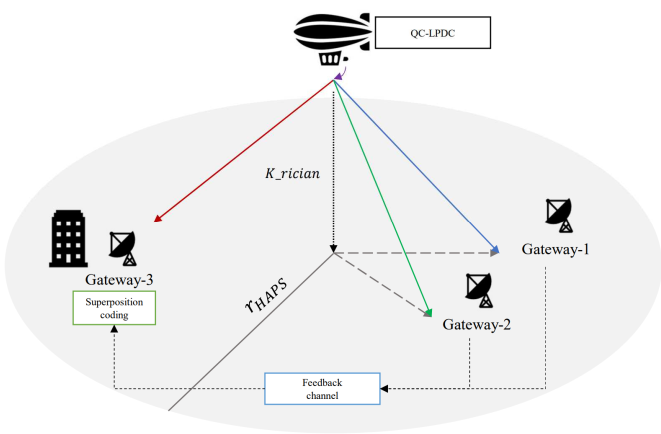

Fig. 1 The HAPS communication model uses NOMA for three gateways.

We proposed a communication system that connects a HAPS to a gateway, using power-domain NOMA for gateway differentiation. Fig. 1 shows the communication system, where the HAPS sends different binary information through a feedback channel from the gateway. Each gateway receives the signal with interference data but uses SIC to separate and recover the desired information [24]. We also explain the details of our method, as shown in Fig. 2. In the first step, we generated random bits for each user and encoded them using QC-LDPC codes with a specified generator matrix. We modulated the encoded bits using binary phase-shift keying (BPSK) and performed SPC to combine the signals from different users. SPC is a technique that uses different users' signals with varying power levels to form a single signal.

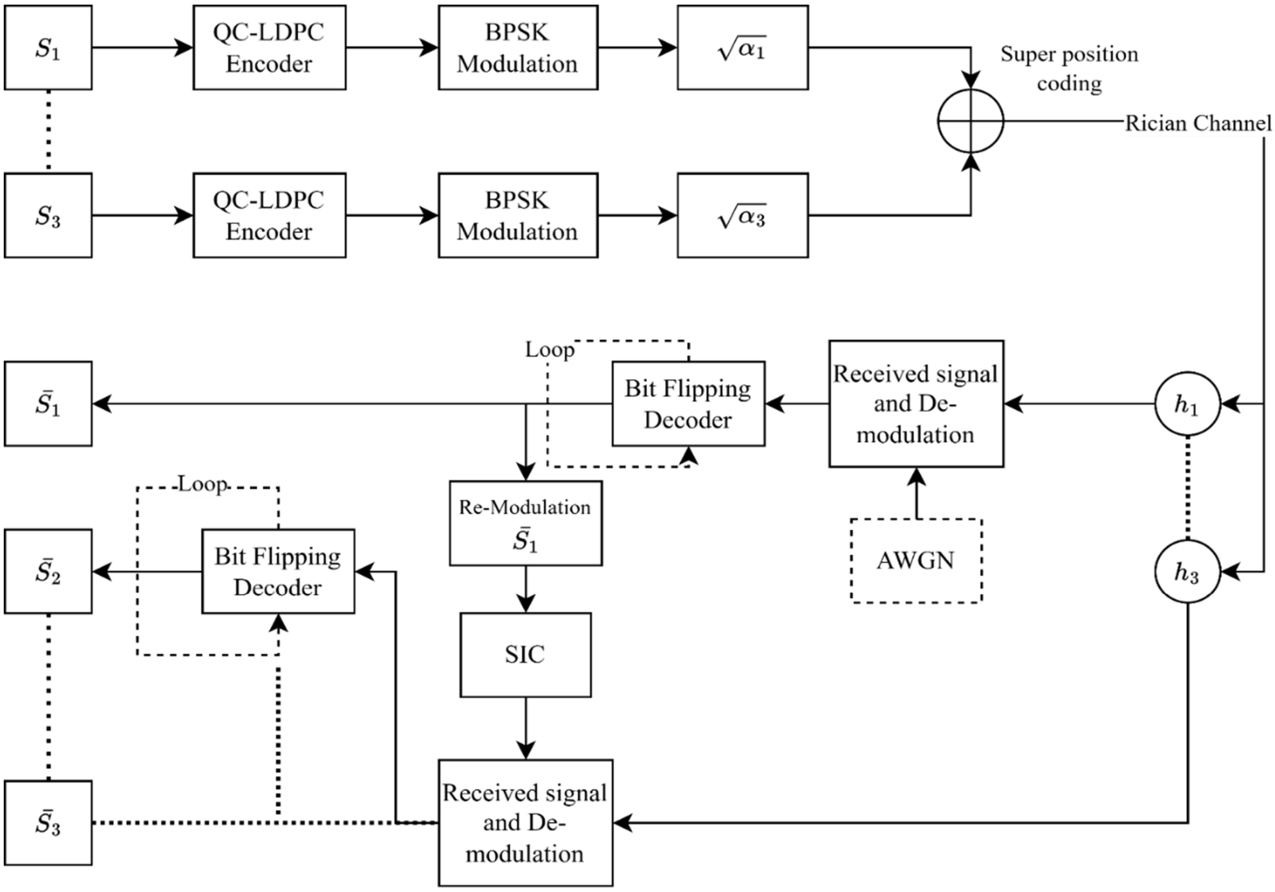

Fig. 2 Diagram block QC-LPDC for NOMA in HAPS communications.

The second step for the diagram block is the channel model for HAPS. We added noise samples with a zero mean and unit variance to the transmitted signal. We calculated the path loss and the total loss due to the distance and the antenna gains of the HAPS and the gateways. We generated Rician fading samples with a specified mean and variance and multiplied them with the transmitted signal. Rician fading is a type of channel fading that models the line-of-sight and the scattered components of the signal. We then relayed the signal to the gateways through the wireless channel.

The last step is the receiver side, which is more complex than the channel model and transmitter. We demodulated the received signal using BPSK and performed SIC to decode the signals from different users. SIC is a technique that subtracts the stronger users' signals to decode the weaker ones' signals. We decoded the received bits using a bit-flipping algorithm and compared them with the original bits to calculate the BER for each user and each SNR value. BER is a measure of the number of transmission errors.

A. Encoder Strategy

Before transmitting information, an encoder known as QC-LDPC was employed to generate a codeword. The codeword was constructed using a generator matrix (G) and a bit information (s), as illustrated in the following p that circular permutation matrix [28]:

$$G = \begin{bmatrix} p^{11} & \cdots & p^{1k} \\ \vdots & \ddots & \vdots \\ p^{j1} & \cdots & p^{jk} \end{bmatrix} \tag{1}$$

To explain the process of the circular permutation matrix, we use the pseudocode shown in Algorithm 1. The pseudocode provided is a function that generates an LDPC code using a quasi-cyclic QC construction algorithm. The function takes five inputs and returns two outputs. Here is a short explanation of the inputs:

- *bitpercol*: the number of bits per column in the base matrix,
- *bitperbar*: the number of bits per row in the base matrix,
- m: the number of bits in the information source,
- g_1: the expected girth of the bipartite graph,
- s: the information source vector of length m,

and for output:

- H: the parity-check matrix of size $(n-k) \times n$, where n is the code length and k is the dimension,
- c: the codeword vector of length n, obtained by multiplying s with the generator matrix.

Algorithm 1: Generator matrix QC-LDPC.

Function *gen_ldpc_qc*(bitpercol, bitperbar,m,g1,s):
    Initialize structures and variables;
    Create the base matrix g_{base};
    Construct the generator matrix G using cyclic shifts of g_{base};
    Initialize variables for shift values and counters;
    for *each group in* G **do**
        Find connections and perform shift operations;
        for *each row in the group* **do**
            Find connected nodes and perform selection;
            if *(selection is successful)* **then**
                Update connections and counters;
            else
                Handle unsuccessful column connection;
                Terminate if needed
            end
        end
    end
    Construct the parity-check matrix H from G ;
    Perform Gaussian elimination on H to create a systematic form H_{sys};
    Compute the codeword c by multiplying s with G ;
    return H and c;
end

We obtained the codeword by multiplying the generator matrix with the bit information. The protected bit with a parity-check generator is reliable and resists channel noise and interference, as shown below.

$$c = G \cdot s \, . \tag{2}$$

We used BPSK modulation to modulate the signal in the simulation. BPSK signal had two phases, one for each bit value. A bit value of one made the signal positive, while a bit value of zero made the signal negative. The following example shows how BPSK modulation works:

$$m_n = \begin{cases} 1, c = 1 \\ 0, c = -1 \end{cases} \tag{3}$$

B. Channel Rician

In the channel modeling process, K-Rician was used to represent the channel for each user, including a line of sight (LOS) component and a fading component, as shown below.

$$h_n = \sqrt{\frac{K}{1+K}} \cdot \overline{h} + \sqrt{\frac{1}{1+K}} \cdot \overline{h_w}, \tag{4}$$

where the LOS component is represented by $\sqrt{\frac{1}{1+K}} \cdot \overline{h}$, while the fading component is represented by $\sqrt{\frac{1}{1+K}} \cdot \overline{h_w}$. Here, K is the Rician K-factor, whose value ranges from 0 to ∞. The channel becomes more deterministic when K is higher, as the K-factor indicates the energy ratio in the fixed LOS component to the energy in the random scattering paths (i.e., the fading component). In brief, the proposed channel model consists of a fixed component (LOS) and a random component (fading), and the K-factor is a critical parameter that determines the degree of determinism in the channel.

A common technique for power allocation in wireless systems is static power allocation (SPA). In this study, power allocation (α_n) The distance between the ground station and HAPS was used to determine each information signal. The distance was calculated using the angular elevation, which resulted in the computation of a K-factor value. The signal was then assigned power allocation accordingly, and its performance in the channel was evaluated, as shown in equation 5.

$$x_n = \sqrt{\alpha_n} \cdot m_n \cdot h_n, \tag{5}$$

where the power allocation factor must be equal to the one as follows.

$$\textstyle\sum_{n=1}^{N} \alpha_n = 1 \tag{6}$$

where N is the number of users.

C. Decoder strategy

After determining the power allocation for each user, the information signals are encoded and multiplexed using SPC. This method superimposes all signals and transmits them to HAPS simultaneously. We assume a coherent time in this simulation and neglect delays during the SPC process. Upon receiving the signals at HAPS, we use mathematical models to analyze the received signals, such as:

$$y = \textstyle\sum_{n=1}^{N} x_n + \sigma, \tag{7}$$

where σ is additive white Gaussian. We assume that HAPS has access to the feedback channel information, which enables it to sort the channel values in descending order ($H_1 > H_2 > \cdots > H_N$). We used re-modulation to optimize the SIC decoding strategy for the signals that are correctly decoded. The demodulation process begins with the first user with the highest channel value and power allocation. We map a positive signal to a bit one (1) and a negative signal to a bit zero (0), as shown in the equation:

$$\bar{x}_n = \begin{cases} y \geq 0, \overline{m_n} = 1 \\ y < 0, \overline{m_n} = 0 \end{cases}. \tag{8}$$

The demodulation process started with the signal from the user with the highest channel value and power allocation. After extracting the bits of information, we re-modulate them using BPSK modulation with the corresponding power allocation. We then subtract the re-modulated signal from the superimposed signal and repeat the process for the remaining users in descending order of their power allocation. The SIC process is mathematically modelled as follows [29].

$$\begin{aligned} \bar{x}_{n-1} = y - \big[\big(remod(\bar{x}_1) \cdot \sqrt{\alpha_1} \cdot h_1 \big) \cdots \\ - \big(remod(\bar{x}_{n-1}) * \sqrt{\alpha_{n-1}} \\ \cdot h_{n-1} \big) \big] \end{aligned} \tag{9}$$

Once the received signal has been demodulated, we apply the bit-flipping decoding technique to extract the information. Let H be the parity-check matrix of the code, $\bar{x}$ is the received signal, and $\bar{s}$ is the estimated message after decoding. Then, the bit-flipping decoding algorithm can be represented by pseudocode, as shown in Algorithm 2. To obtain the BER, we compare the transmitted and received bit information. The BER is calculated as the ratio of the number of error bits (N_e) to the number of transmitted bits (N_t), as shown in the following equation.

$$P_e = \frac{N_e}{N_t}. \tag{10}$$

Algorithm 2: Bit flipping decoding.

Function *bitflipdec*($\bar{x}, H$,loop):
    Initialize c_i with $\bar{x}$;
    Initialize q_{ij} with H and c_i;
    for $n = 1$ *to* loop **do**
        Perform horizontal step;;
        Update r_{ji} using q_{ij} and H;
        Perform vertical step:;
        Update r_{ji} , r_0, r_1, and $\hat{v}$;
        Perform bit decoding;
        Set y to $\hat{v}$;
        Check for convergence;
        if $H \cdot y^T$ *is all zeros* **then**
            Break;
        end
    end
    return y ;
end

The parity-check matrix H is used to check whether the estimated message $\bar{s}$ satisfies all the parity-check equations. If not, the algorithm iteratively flips the bits in $\bar{s}$ that violate the parity-check equations until a valid codeword is obtained. We also utilized various parameters to support our extensive simulation. Three gateways were deployed to expand communication for end-users, each with a distinct channel gain and power allocation determined by location. Moreover, the simulation parameters were based on the ITU-R downlink system and are detailed in Table 1.

TABLE I
SIMULATION PARAMETERS

Parameter	Value
Frequency Operation	48 GHz
Transmitted power	20 dBW
Gain antenna	46 dBi
Number of bits	10000
Number of stations	3
HAPS altitude	21 km
Channel model	K-Rician
Code-rate	0.5
Power allocation	0.8, 0.15, 0.05

III. RESULT AND DISCUSSION

This section presents the simulation outputs obtained by testing the parameters relevant to the research problem. The test parameters considered in this study include SNR and BER. BER is a metric used to evaluate the quality of the transmitted data by measuring the number of bit errors per total number of bits transmitted. In this simulation, the maximum BER considered is 10^{-3}, corresponding to only one-bit error out of 1000 bits transmitted.

A. Uncoded Information of HAPS

Fig. 3 presents the simulation results without parity check for three gateway scenarios. The figure shows that the third user achieves the BER target of 10^{-3} and needs more than 30 dB of SNR. On the other hand, the second gateway requires around 25.5 dB of SNR to obtain the target BER. The first user achieves the best performance at 24.5 dB of SNR due to the first decoding at the receiver. While NOMA is suitable for maximizing bandwidth occupancy, it also faces challenges like domino error. When the first gateway has wrong decoded information, it will affect the following user's performance. Therefore, all the gateways cannot have the same result, and the power allocation affects the overall system performance.

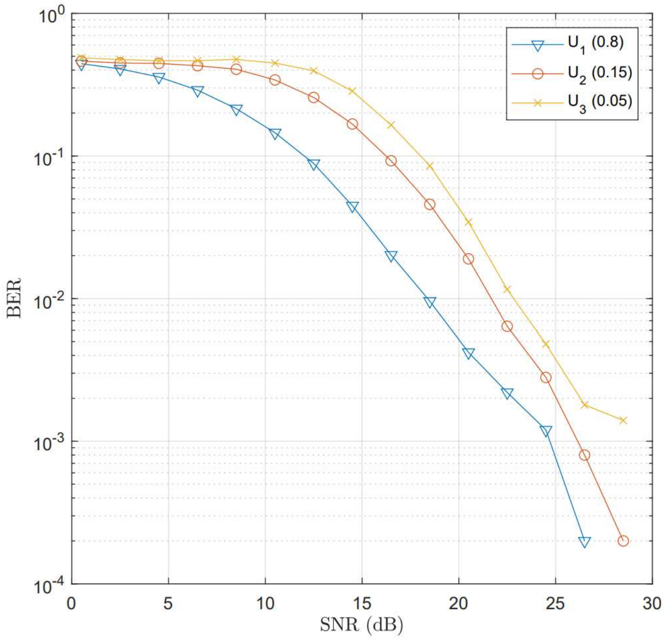

Fig. 3 Simulation Result Performance Uncoded information in HAPS NOMA

B. QC-LDPC information of HAPS

Fig. 4 also shows that the system's performance is greatly improved using QC LDPC with parity check. The decoding process in the receiver bit-flipping improves the system's performance. The third user can achieve the BER target with more than 28 dB of SNR. In addition, the second gateway requires around 25 dB of SNR to obtain the target BER. The first user still achieves the best performance, with an SNR of 22 dB, due to the first decoding process at the receiver.

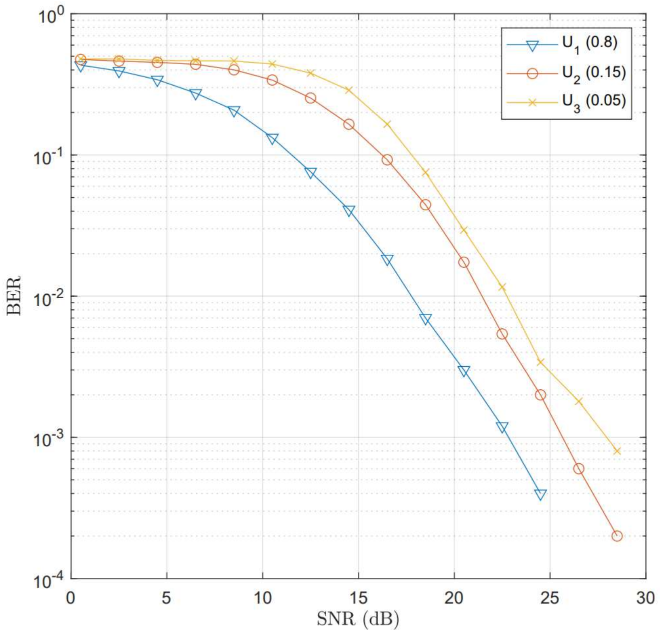

Fig. 4 Simulation result performance QC-LDPC in HAPS NOMA

The results show that NOMA with QC LDPC outperforms NOMA without a parity check regarding bit error rate. The parity check is an effective technique to enhance the system's performance by reducing the bit errors. However, the system's performance depends on each gateway's power allocation and channel gain, which are not optimized in this study. Therefore, future work should focus on finding the optimal power allocation and channel gain for each gateway to achieve the best performance while meeting the BER requirement.

C. Comparison of the Performance of CODING NOMA

The analysis demonstrates that QC-LDPC can achieve a lower SNR for the same BER as uncoded NOMA, as shown in Fig. 5. This indicates that LDPC can improve performance in low-received power scenarios. The second gateway does not differ much between LDPC and uncoded NOMA due to its location and power allocation. However, the third gateway shows a worse performance with LDPC due to its lowest power allocation and the effect of SIC. On the contrary, the first gateway shows a significant performance improvement with LDPC compared to uncoded NOMA [23].

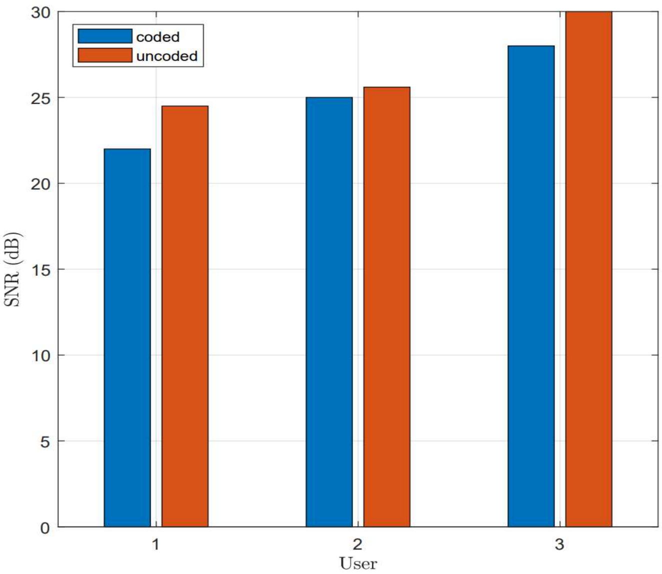

Fig. 5 SNR comparison for HAPS NOMA in various gateway circumstances between QC-LDPC and uncoded data

The simulation results demonstrate that QC-LDPC can improve the reliability and efficiency of the NOMA system, especially in scenarios where the power allocation is not balanced, or the channel gains vary significantly. However, QC-LDPC decoding requires more computational resources than uncoded NOMA, which could be a limiting factor in some practical implementations. Therefore, carefully analyzing the system requirements and constraints is necessary to determine whether QC-LDPC suits a specific NOMA system. Moreover, from our knowledge, our work is the first to investigate channel coding in power domain NOMA for HAPS communication in Rician transmission, as previous studies [24] and [30] only considered uncoded NOMA and not simulated sending information.

IV. Conclusion

This research evaluated the performance of the NOMA system with and without QC-LDPC codes in three different gateway scenarios. The simulation results revealed that the QC-LDPC codes can substantially enhance the overall system performance by lowering the SNR needed to achieve the same target BER. For example, user 1 achieved a 6.67% SNR reduction with QC-LDPC codes compared to uncoded NOMA, while user 3 achieved a 10.20% SNR reduction. The third gateway scenario, with the lowest power allocation and SIC in the last gateway, showed the most remarkable improvement with QC-LDPC codes. However, each gateway's power allocation and location influence the system's performance. NOMA is a promising technology for maximizing bandwidth utilization, but it also faces challenges like domino error, which can degrade the performance of subsequent users. Therefore, it is essential to carefully design and optimize each gateway's power allocation and location to ensure optimal system performance. Overall, this research provides insights into the performance of NOMA systems and suggests potential areas for future research and improvement.

Acknowledgment

We thank the Atma Jaya Catholic University of Indonesia for collecting data and Telkom University for enhancing channel coding.

References

[1] G. K. Kurt *et al.*, “A Vision and Framework for the High Altitude Platform Station (HAPS) Networks of the Future,” *IEEE Communications Surveys & Tutorials*, vol. 23, no. 2, pp. 729–779, 2021, doi: 10.1109/COMST.2021.3066905.

[2] K. Mershad, H. Dahrouj, H. Sarieddeen, B. Shihada, T. Al-Naffouri, and M.-S. Alouini, “Cloud-Enabled High-Altitude Platform Systems: Challenges and Opportunities,” *Frontiers in Communications and Networks*, vol. 2, 2021, doi: 10.3389/frcmn.2021.716265.

[3] S. Alfattani, A. Yadav, H. Yanikomeroglu, and A. Yongacoglu, “Resource-Efficient HAPS-RIS Enabled Beyond-Cell Communications,” *IEEE Wireless Communications Letters*, vol. 12, no. 4, pp. 679–683, 2023, doi: 10.1109/LWC.2023.3239210.

[4] E. Erdogan, O. B. Yahia, G. K. Kurt, and H. Yanikomeroglu, “Optical HAPS Eavesdropping in Vertical Heterogeneous Networks,” *IEEE Open Journal of Vehicular Technology*, vol. 4, pp. 208–216, 2023, doi:10.1109/OJVT.2022.3232272.

[5] A. Traspadini, M. Giordani, and M. Zorzi, “UAV/HAP-Assisted Vehicular Edge Computing in 6G: Where and What to Offload?,” in *2022 Joint European Conference on Networks and Communications & 6G Summit (EuCNC/6G Summit)*, IEEE, Jun. 2022, pp. 178–183. doi: 10.1109/EuCNC/6GSummit54941.2022.9815734.

[6] A. Andreadis, G. Giambene, and R. Zambon, “Role of UAVs and HAPS for IoT-based Monitoring in Emergency Scenarios,” in *International Conference on Information and Communication Technologies for Disaster Management (ICT-DM)*, 2023, pp. 1–8. doi:10.1109/ICT-DM58371.2023.10286916.

[7] Z. Jia, Q. Wu, C. Dong, C. Yuen, and Z. Han, “Hierarchical Aerial Computing for Internet of Things via Cooperation of HAPs and UAVs,” *IEEE Internet Things J*, vol. 10, no. 7, pp. 5676–5688, 2023, doi: 10.1109/JIOT.2022.3151639.

[8] H. Cao, G. Yu, and Z. Chen, “Cooperative Task offloading and Dispatching Optimization for Large-scale Users via UAVs and HAP,” in *IEEE Wireless Communications and Networking Conference (WCNC)*, 2023, pp. 1–6. doi: 10.1109/WCNC55385.2023.10118722.

[9] S. A, K. S, L. I. N. H, and O. H, “Propagation Loss Model of Human Body Shielding in HAPS Communications,” in *International Symposium on Antennas and Propagation (ISAP)*, 2021, pp. 65–66. doi: 10.23919/ISAP47053.2021.9391216.

[10] A. Yılmaz, N. Yılmaz, G. Kalem, and M. A. Durmaz, “Path Gain and Channel Capacity for HAP-to-HAP Communications,” in *2023*

International Conference on Unmanned Aircraft Systems (ICUAS), IEEE, Jun. 2023, pp. 305–312. doi:10.1109/ICUAS57906.2023.10155817.

[11] T. V Nguyen, H. D. Le, and A. T. Pham, "On the Design of RIS–UAV Relay-Assisted Hybrid FSO/RF Satellite–Aerial–Ground Integrated Network," *IEEE Trans Aerosp Electron Syst*, vol. 59, no. 2, pp. 757–771, 2023, doi: 10.1109/TAES.2022.3189334.

[12] A. Noordin, M. A. M. Basri, Z. Mohamed, and A. F. Z. Abidin, "Modelling and PSO fine-tuned PID control of quadrotor UAV," *International Journal on Advanced Science Engineering Information Technology*, vol. 7, no. 4, pp. 1367–1373, 2017, doi:10.18517/ijaseit.7.4.3141.

[13] Y. Zhang, M. A. Kishk, and M.-S. Alouini, "HAP-enabled Communications in Rural Areas: When Diverse Services Meet Inadequate Communication Infrastructures," *IEEE Open Journal of the Communications Society*, 2023, doi:10.1109/OJCOMS.2023.3318836.

[14] S. Alfattani, W. Jaafar, H. Yanikomeroglu, and A. Yongaçoglu, "Multimode high-altitude platform stations for next-generation wireless networks: Selection mechanism, benefits, and potential challenges," *IEEE Vehicular Technology Magazine*, 2023, doi:10.1109/MVT.2023.3289630.

[15] M. Kırık, N. A. Abusanad, and H. Arslan, "Inter-HAP Based Geometrical 3-D Channel Model Operating at 28 to 60 GHz for Future 6G Non-Terrestrial Networks," in *IEEE Wireless Communications and Networking Conference (WCNC)*, 2023, pp. 1–5. doi:10.1109/WCNC55385.2023.10118591.

[16] H. Vu, T. L. Le, V. G. Nguyen, and T. H. Dinh, "Semantic regions segmentation using a spatio-temporal model from an UAV image sequence with an optimal configuration for data acquisition," *Journal of Information and Telecommunication*, vol. 2, no. 2, pp. 126–146, Apr. 2018, doi: 10.1080/24751839.2017.1390654.

[17] S. Fei *et al.*, "UAV-based multi-sensor data fusion and machine learning algorithm for yield prediction in wheat," *Precis Agric*, vol. 24, no. 1, pp. 187–212, 2023, doi: 10.1007/s11119-022-09938-8.

[18] F. T. Teshome, H. K. Bayabil, G. Hoogenboom, B. Schaffer, A. Singh, and Y. Ampatzidis, "Unmanned aerial vehicle (UAV) imaging and machine learning applications for plant phenotyping," *Comput Electron Agric*, vol. 212, p. 108064, Sep. 2023, doi:10.1016/j.compag.2023.108064.

[19] H. Omote, S. Kimura, H. Y. Lin, and A. Sato, "HAPS propagation loss model for urban and suburban environments," in *International Symposium on Antennas and Propagation (ISAP)*, 2021, pp. 681–682. doi: 10.23919/ISAP47053.2021.9391285.

[20] M. Indoonundon and T. P. Fowdur, "Overview of the challenges and solutions for 5G channel coding schemes," *Journal of Information and Telecommunication*, vol. 5, no. 4, pp. 460–483, 2021, doi:10.1080/24751839.2021.1954752.

[21] C. E. Kement *et al.*, "Sustaining dynamic traffic in dense urban areas with high altitude platform stations (HAPS)," *IEEE Communications Magazine*, vol. 61, no. 7, pp. 150–156, 2023, doi:10.1109/MCOM.001.2200584.

[22] M. S. Alamgir and B. Kelley, "Fixed Wing UAV-based Non-Terrestrial Networks for 5G millimeter wave Connected Vehicles," in *IEEE 13th Annual Computing and Communication Workshop and Conference (CCWC)*, 2023, pp. 1167–1173. doi:10.1109/CCWC57344.2023.10099281.

[23] O. Abbasi and H. Yanikomeroglu, "A Cell-Free Scheme for UAV Base Stations with HAPS-Assisted Backhauling in Terahertz Band," in *IEEE International Conference on Communications*, 2022, pp. 249–254. doi: 10.1109/ICC45855.2022.9838511.

[24] H. Shuai, K. Guo, K. An, Y. Huang, and S. Zhu, "Transmit Antenna Selection in NOMA-Based Integrated Satellite-HAP-Terrestrial Networks With Imperfect CSI and SIC," *IEEE Wireless Communications Letters*, vol. 11, no. 8, pp. 1565–1569, 2022, doi:10.1109/LWC.2022.3165710.

[25] D. Wang, M. Wu, Y. He, L. Pang, Q. Xu, and R. Zhang, "An HAP and UAVs Collaboration Framework for Uplink Secure Rate Maximization in NOMA-Enabled IoT Networks," *Remote Sens (Basel)*, vol. 14, no. 18, p. 4501, 2022, doi: 10.3390/rs14184501.

[26] S. M. Fauzi Aulia, K. Anwar, and N. Andini, "Channel Coding for Multimedia Transmission on High-Speed Flying Devices," *Int J Adv Sci Eng Inf Technol*, vol. 11, no. 4, 2021, doi:10.18517/ijaseit.11.4.14105.

[27] X. Liu, H. Liu, C. Liu, and Y. Luo, "Time-Varying Communication Channel High Altitude Platform Station Link Budget and Channel Modeling," *Information*, vol. 9, no. 9, p. 210, 2018, doi:10.3390/info9090210.

[28] B. Pamukti, F. Arifin, and N. M. Adriansyah, "Low Density Parity Check Code (LDPC) for Enhancement of Visible Light Communication (VLC) Performance," in *International Seminar on Application for Technology of Information and Communication (iSemantic)*, IEEE, 2020, pp. 262--266. doi:10.1109/iSemantic50169.2020.9234285.

[29] V. W. Mahyastuty, I. Iskandar, H. Hendrawan, and M. S. Arifianto, "Medium Access Control Protocol for High Altitude Platform Based Massive Machine Type Communication," *Journal of ICT Research and Applications*, vol. 16, no. 2, pp. 123–137, 2022, doi:10.5614/itbj.ict.res.appl.2022.16.2.2.

[30] S. ul Hassan, T. Mir, S. Alamri, N. A. Khan, and U. Mir, "Machine Learning-Inspired Hybrid Precoding for HAP Massive MIMO Systems with Limited RF Chains," *Electronics (Basel)*, vol. 12, no. 4, p. 893, Feb. 2023, doi: 10.3390/electronics12040893.